Carbon Nanotube Transistors for Biosensing Applications

G. Gruner
Department of Physics
University of California Los Angeles
Los Angeles, CA 90095
and
Nanomix Inc.
Emeryville CA 94508

ABSTRACT

Electronic detection of biomolecules is gradually emerging as effective alternative of optical detection methods. We describe transistor devices with carbon nanotube conducting channels that have been used for biosensing and detection. Both single channel field effect transistors and devices with network conducting channels have been fabricated and their electronic characteristics examined. Device operation in (conducting) buffer and in a dry environment - after buffer removal - is also discussed. The devices readily respond to changes in the environment, such effects have been examined using gas molecules and coating layers with specific properties. Finally the interaction between devices and biomolecules will be summarized, together with the electronic monitoring of biomolecular processes.

1.INTRODUCTION

Most of the biological sensing techniques rely largely on optical detection principles. The techniques are highly sensitive and specific, but are inherently complex, require multiple steps between the actual engagement of the analyte and the generation of a signal, multiple reagents, preparative steps, signal amplification, and complex data analysis. Single molecule detection, while demonstrated in a few cases, requires the application of optical probe molecules that may change the functionality of the biomolecules in question. Electronic detection, utilizing nanoscale devices offers opportunities for two reasons. The first is size compatibility. Thanks to recent advances in nanoscale materials, we are now able to construct electronic circuits in which the component parts are comparable in size to biological entities, thus ensuring appropriate size compatibility between the detector and the detected species. Some length scales illustrate this observation: single cells are approximately 1 micron in size, viruses are approximately 100 nanometers, while individual proteins are on the order of 10 nanometers, and the diameter of the DNA duplex is approximately 1 nanometer. Compare this with the size range for nanostructures: optical lithography-based nanowire fabrication reaches down to 100 nm, the size of a typical virus. E-beam fabrication has the current limit of approximately 30nm, and innovative printing technologies also reach this length scale. The typical cross section of fabricated semiconductor nanowires is currently on the order of 10x10 nanometers, the approximate size of a protein, and the diameter of single-wall carbon nanotubes – naturally occurring hollow cylinders - is in the 1 nanometer range, the diameter of the DNA duplex. The second argument for developing electronic detection schemes is due to the fact that most biological processes involve electrostatic interactions and charge transfer, this allows electronic detection, and the merging of biology and electronics.

Because of the rich potential of biosensors[1] and bioelectronics,[2] recent research has focused on the interactions between biomolecules and inorganic systems. The integration of biological processes and molecules with fabricated structures also offers both electronic control and sensing of biological systems and biologically electronic driven nanoassembly[3]. As a specific example, carbon nanotubes have been suggested for use as prosthetic implants in nervous systems[4], this goal requires the integration of fully functioning biological and nanoelectronic systems. Thus far, researchers have used organic and inorganic chemistry to attach proteins[5], DNA[6], and lipids[7] to nanotubes, nanowires, and nanocrystals. In such bottom-up construction, a single biological species is integrated with a single type of nanostructure, usually in solution. To move towards functional devices, further processing is required, which may damage the biological molecules. Alternatively, to make more complex biological structures requires that biological activity be preserved despite the presence of the nanostructures. As a result, the nanostructures have served only as mechanical supports, without electronic functionality[2].

Nanotubes have been functionalized to be biocompatible and to be capable of recognizing proteins.[8-11] Often, this functionalization has involved non-covalent binding between a bi-functional molecule and a nanotube to anchor a bio-receptor molecule with a high degree of control and specificity. The unique geometry of nanotubes has also been used to modify nanotube-protein binding. The conformational compatibility, driven by both steric and hydrophobic effects, between proteins and carbon nanotubes has been examined using streptavidin and other proteins. For example, streptavidin has been crystallized in a helical conformation around multiwalled carbon nanotubes.[12] Conversely, the tendency of biological materials to self-organize has been used to direct the assembly of nanotube structures.[13]

Field effect transistors (FET's) fabricated using semiconducting single-wall carbon nanotubes (SWNTs) as the conducting channel (nanotube FET's, NTFET's) have been extensively studied[14,15], and the electronic characteristics of the devices are well explored and reasonably well understood. The devices have been found to be sensitive to various gases[16,17], such as ammonia, and thus can operate as sensitive chemical sensors. We[18,19], and some other groups[20] have explored electronic detection of chemical species in a liquid environment. We have also found that these devices are extremely sensitive, and are able to detect a single molecule both in air and in a (conducting and non-conducting) liquid environment. Such devices are also promising candidates for electronic detection of biological species. Initial studies, performed by us[21-23], indicate that the extreme sensitivity of the devices may - after improvement of the device characteristics, such as noise, and in an appropriately fabricated environment - lead to single biomolecule detection and to real-time monitoring of conformational changes of biomolecules.

2. DEVICE ARCHITECTURES

Two different device architectures, both utilizing carbon nanotubes that connect the source and drain electrodes the source and gate electrodes have been developed. In one device architecture a single nanotube channel connects the source and the drain, in a configuration that is shown in **Fig.1**. Such devices have been utilized in the bio-sensing area but there is substantial variation between the different devices that are fabricated. In an alternative device architecture, the devices contain a random array of nanotubes functioning as the conducting channel, as shown in **Fig.2**. Current flows along several conducting channels that determine the overall device resistance. The construction has several advantages. Device operation depends on the density of nanotubes. For a dense array screening of the gate voltage by the conducting nanotubes is important, in a fashion similar to gate voltage screening due to a metal layer deposited on the device. For a rarified array such screening is not important and the array can serve as the source-to-drain conducting channel. It is expected that arrays close to, and on the conducting side of the two dimensional percolation limit will have appropriate transistor characteristics. Under such circumstances screening effects are expected to be small, but conduction is still provided by the nanowire network. In both cases the parameter that is used for detection is the so-called device characteristic (DC), the dependence of the source-drain current, I_{sd} (for a fixed source-drain voltage V_{sd}) on the gate voltage V_G, a typical DC is displayed on **Fig. 2.** As a rule the devices also display a hysteresis, due to mobile ions at the surface of the devices. In the following such hysteresis

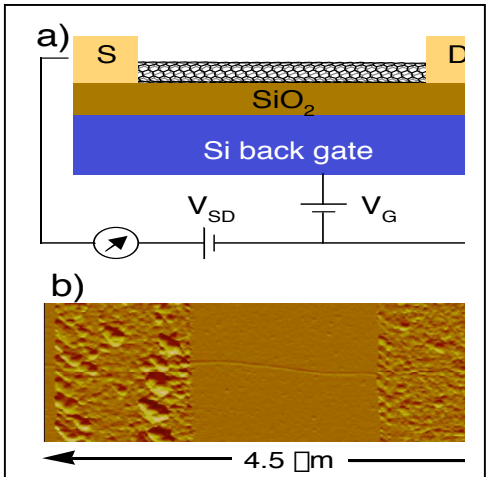

Fig.1. a) Schematic of a single nanotube channel transistor (NTFET). b) AFM image of a NTFET device. The thin horizontal line is the nanotube connecting the source and drain.

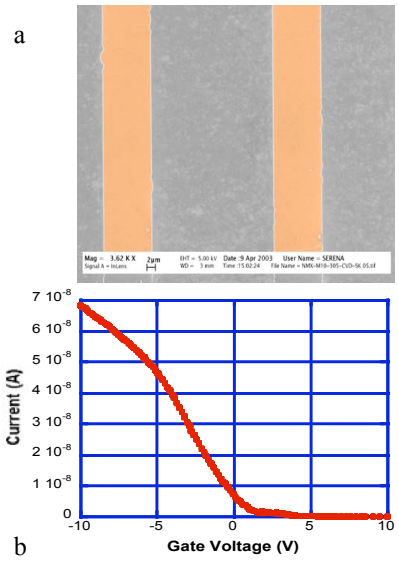

Fig 2. Nanotube network transistor. a) AFM image of the device, b) the source-drain current (referred to as the "device characteristics, DC") versus the gate voltage.

will be shown only if relevant to the observations, otherwise only gate voltage sweeps in one direction – as in **Fig. 2b** - with be displayed.

3. DETECTION SCHEMES

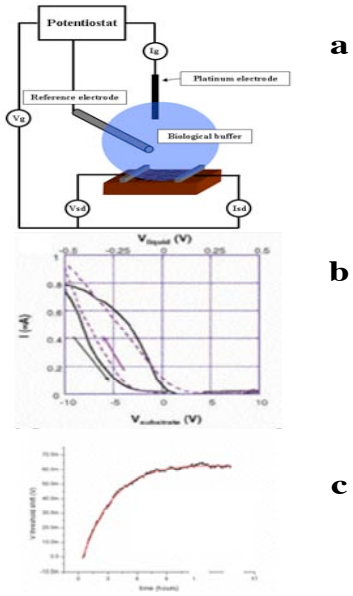

Fig 3. a) Arrangement for "liquid gating" as described in the text. b) Device characteristics for both "liquid gating" (lower scale) and "bottom gating", (upper scale). Note the different Vg scales in the two cases. c) Shift of the DC versus time during incubation with streptavidin.

Several alternative detection schemes can be employed for biosensing applications. The presence of an immobilized biomolecule, or the completion of a reaction between biomolecules (such as a ligand-receptor binding for example) can be followed by examining the change of the device characteristics after the biomolecule is immobilized, the reaction completed and the buffer is removed. The DC is measured in a conventional configuration, applying the bottom gate (called "bottom gating") as shown in **Fig.2b**. This is appropriate if the mere presence of the biomolecule, or the completion of the biological reaction is examined only, and thus may be an appropriate method for a variety of biotechnology applications. It is much preferable however to monitor the biological processes that take place in an appropriate buffer environment. Real-time signal acquisition and analysis may have significant impact on the biological sciences for several reasons. First, the time scales for biological processes may be directly measured. The time for a protein to undergo conformational changes, or DNA duplex formation and its complement to form a duplex, could be directly measured. Secondly, the electronic data may lead to seek electronic signatures specific to a biological process. For example, if the binding of different antigens to an antibody each results in a particular electronic signature, then the different antigens may be distinguished from each other. This could dramatically alter the landscape of biological sensing, and aid the development of practical biosensors by solving the problems of false positives and poor cross-sensitivities. Biomolecules undergo a variety of fluctuations and conformational changes that span several orders of magnitude. Picosecond time scales characterize intramolecular vibrations[24], with anharmonic relaxations[25] on the order of nanosecond. Protein collapse occurs at milliseconds to seconds[26-31]. The internal time constant of our devices is on the order of microseconds, allowing signal processing at time scales exceeding this limit.

The fact that physiological buffer is conducting offers a detection scheme[32], alternative to "bottom gating". An electrode is applied to the liquid and and I_{sd} is measured as function of the voltage on the electrode, as depicted in **Fig.3a**. Several precautions have to be made. Electrochemical reactions may take place for large gate voltages, these can be identified (and avoided) by monitoring the current between the gate and the conducting channel. The source and drain electrodes – and all the conducting leads have to be isolated from the buffer in order to avoid non-desirable reactions. A typical DC for both "liquid gating" and "bottom gating" is shown in **Fig.3b**. The two configurations result in a similar DC if an appropriate scaling of the x-axis is performed, this scaling is due to the different dielectric layer in the two cases: an oxide insulating layer for bottom gating and a hydration layer in case of "liquid gating". Monitoring the change of the DC versus time, as shown in **Fig 3c** allows the real time monitoring of protein attachment to the device – and a variety of biological processes for that matter.

4. INTERACTION OF THE DEVICES WITH THE ENVIRONMENT

The transistor configuration is different from usual transistor configurations: here the most sensitive element of the device, the conducting channel is open to the environment. In addition because of the tubular structure, all the current flows at the surface of the channel, in direct contact with the environment. As the result these devices are extremely

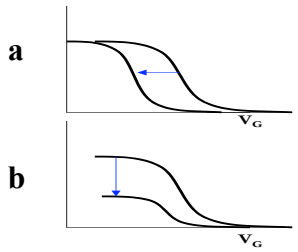

Fig.4. Change of the transistor device characteristic (DC) in the presence of an adsorbed species S. a) electron transfer from S to the nanotube, b) potential scattering of charge carriers on the potential created by S.

sensitive to environmental factors, the presence of different chemical and biological species in the vicinity of the device. The interaction of devices with various inorganic species has been explored in detail, such experiments serve as useful benchmarks for the effects that are observed when the environment is modified. Both exposure to gases and to coating layers have been studied.

Consider a molecule in the vicinity (usually at the surface) of the nanotubes that forms the conducting channel. The effect of such molecule may be similar to the effect of an impurity in a conventional semiconductor with two possible consequences. There may be a charge transfer form the molecule to the nanotube channel, and the molecule may act as a scattering potential. The consequences of the two are different: a charge transfer to the nanotube shifts the DC towards more positive (electron donation form the molecule to the nanotube) or negative (hole donation) gate voltages. In contrast, a molecule may act as a scattering center leading to the decrease of the mobility, thus suppressing the DC without a shift – such suppression may occur also through a mechanical distortion of the nanotube. The two situations are depicted in **Fig. 4**.Both may occur, and the transistor configuration allows the separation of the two factors, the change of the carrier density and mobility.

4.1. Interactions with gases.

Upon exposure to various gases, one finds a shift of the DC, either left or to the right, towards more negative or positive gate voltages, indicating a charge transfer from or to the nanotube, and the effect has been studied in detail. **Figure 5a** shows the effect for an electron donating (NH_3) and electron withdrawing (NO_2) species in Ref 33 and by us Although the notion that the effect is due to the charge transfer between the molecular species and the carbon nanotubes is not universally accepted, unpublished calculations strongly suggest that this is the case. The response to ammonia has also been studied in water[5], and the shift of the DC is displayed on **Fig. 5b** for different ammonia concentrations. The full line describes of what is expected for weak binding of the NH_3 molecules. Under such circumstances the molecules hop on and off the channel, creating a dynamic equilibrium. The coverage of the devices can be calculated as the function of the NH_3 concentration in the liquid, and assuming that the change (in this case the shift of the DC) is proportional to the coverage, the shift can be calculated as function of the concentration. The full line in **Fig. 5b** represents the calculated dependence – describing to observations to good accuracy. These experiments also confirm that there is a charge transfer from HN_3 to the nanotube channel, with scattering effects (see **Fig. 4**) playing a lesser role.

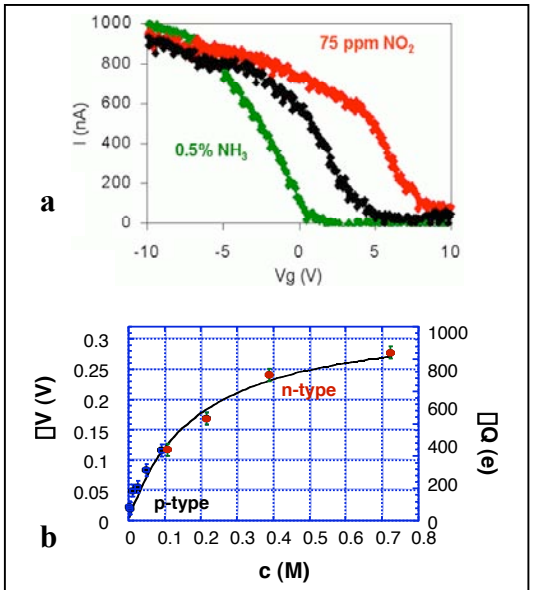

Fig. 5. a) Effect of electron donating NH_3 and electron withdrawing NO_2 on the transistor device characteristic. b) The shift of the device characteristic, □V upon exposure to NH_3 in water, in different NH_3 concentration.

4.2 The effect of polymer coating on the DC.

The devices have also been coated with various, mainly polymer layers in order to change the device characteristic and achieve a desired defined functionality. Both poly(ethylene) glycol (PEG) and poly(ethylene) imine (PIE) have been explored because of their bio-functionality. A PEG layer has little influence of the DC, while PEI dramatically changes the DC. The effect of adsorbed amines on nanotube electronic properties has been studied by several authors[33,34]. The most quantitative measurement has shown that 0.04 electrons per adsorbed amine are donated to semiconducting nanotubes. This charge donation is detected as a shift of the threshold voltage of nanotube transistors towards negative gate voltages. PEI is a highly branched polymer with a molecular weight of about 25,000 and about 500 monomers per chain. About 25% of the amino groups of PEI are primary with about 50% secondary, and 25% tertiary. Deposition of PEI on nanotube devices results in negative shifts in the device threshold voltages indicating

electron transfer to the nanotubes. The amount of charge transfer depends on the number of amino groups in the polymer and their basicity. This has been confirmed by us through the deposition of PEI polymer from different aqueous solutions with different pH values. Computer modeling has been used to evaluate the density of amino groups in adsorbed PEI polymer, with the conclusion that 3-10 amino groups are located on 1 nm^2 of polymer surface area. Because the monomers are small and mobile in the case of the polymer, we assume that the full nanotube circumference is available for adsorption. Thus a 1 μm nanotube adsorbs 23,000 to 75,000 amine groups from PEI.

5. INTERACTIONS BETWEEN THE DEVICES AND BIOMOLECULES.

Because of the rich potential of nanobiotechnology, including biosensors[35] and bioelectronics,[36] recent research has focused on the interactions between biomolecules and inorganic systems. A major goal continues to be the fabrication of structures with proteins immobilized on various functional surfaces, while preserving the biological activity of the proteins.[37,38] A variety of mechanisms have been explored for immobilization, including covalent bonding,[37] hydrophobic interactions, and charge transfer-induced adsorption.[40] The most direct evidence has been provided by scanning force microscopy, which in recent years has been used to measure the strength of protein attachment.[41] Interactions between biomolecules and various surfaces have been widely utilized, and to some extent studied, however the interaction between the surfaces and the biomolecules are less understood. The interrogation of the device characteristics before and after immobilization offers an opportunity of identifying some of these interactions.

5.1. Proteins immobilized on the device

We have used biotinilated bovin serum albumin (BBSA) and similar proteins to examine the interactions, and the SEM images give clear evidence (**Figure 6a**) of nonspecific protein binding to nanotubes in a buffer environment. Note that have the nanotubes do not form part of the electronic device. Such protein immobilization on nanotubes has been observed before by other groups and is by itself not surprising given the good size compatibility of the two entities. We made similar observations for streptavidin and a range of other proteins. These images also confirm a strong binding between the nantubes and proteins. Unlike is the case for ammonia discussed before, once s protein is bound to the nanotubes, it will remain bound to the devices under ambient conditions various contributions to the bindings have been suggested, with hydrophobic interactions as the main source of immobilization. Streptavidin is a tetrameric protein of M_r 64,000[42]. According to electrophoretic measurements, it is electrically neutral at pH values between 6 and 7.2. However, it contains a number of residues with strong side chain bases[42-46]. Each streptavidin monomer has two histidine residues. His-87 is located close to the biotin binding pocket on the "top" and "bottom" of the protein, and His-127 residues lie on the long side of the barrel at the interface between two subunits. Histidine is one of the strongest bases at physiological pH (7.0), and it plays a major role in streptavidin's recognition of biotin[42]. For other important base-containing residues, such as lysine and arginine, only some of the residues have been specifically located in the tertiary structure. Based on those locations that have been identified, we estimate that the external envelope of the protein contains 80 arginine residues and 20 lysine residues, for a total of 100 amine groups.

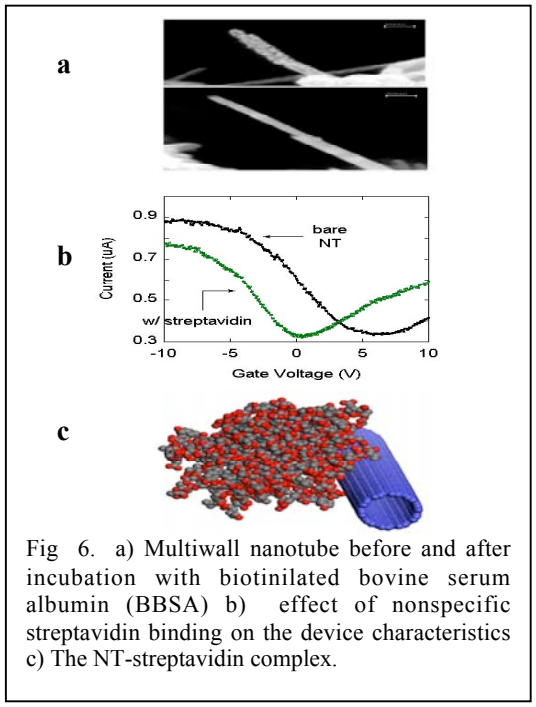

Fig 6. a) Multiwall nanotube before and after incubation with biotinilated bovine serum albumin (BBSA) b) effect of nonspecific streptavidin binding on the device characteristics c) The NT-streptavidin complex.

The observation of a shift of the DC when the devices are "coated" with streptavidin **(Figure 6b**) indicates that charge transfer plays a role in protein adsorption as well. The magnitude of the charge transfer from proteins can be assessed by comparing our simple protein model with measurements using NH_3 and PEI. The specific quantity of charge transferred can be estimated using the calibration provided by measurements of ammonia adsorption, which have found that each adsorbed group donates 0.04 electrons. Given the capacitance of between the nanotube and the gate, the quantity of donated charge can be related to the observed threshold shift. The capacitance depends on the nanotube diameter, and for

a nanotube of diameter 2.4 nm is approximately 500 aF (Rosenblatt et al., 2002). If the 4,000 amine groups are contributed from the adsorbed proteins, with each group donating 0.04 electrons, this represents a quantity Q=17 aC of donated charge. Since the nanotube capacitance to the liquid gate, C, is 500 aF, this donated charge should produce a threshold shift, given by $\Delta V = Q/C$ of -50 mV. By comparison, the observed threshold shift in the presence of a monolayer of protein in buffer is -60±3 mV, in good agreement with the estimated value.

The number of amine groups can also be estimated using a simple model in which roughly spherical proteins cover the top half of the cylindrical nanotube. The proteins are assumed to coat the available nanotube surface with amine groups proportional to the surface area in contact. The nanotube under consideration here has a diameter of 2.4 nm (as reflected in the small bandgap observed in **Fig. 6a),** so that the surface area in contact with each 5 nm protein is $\frac{1}{2} \cdot 2.4 \cdot 5\ \text{nm}^2$. Each protein surface contains 100 amine groups distributed over the 5 nm sphere, so that on average each protein contacts the nanotube with 20 amine groups. Since the proteins are 5 nm in diameter, we assume that 200 proteins are adsorbed on the 1 mm nanotube. Thus the monolayer of adsorbed protein contacts the nanotube with 4,000 adsorbed amine groups.

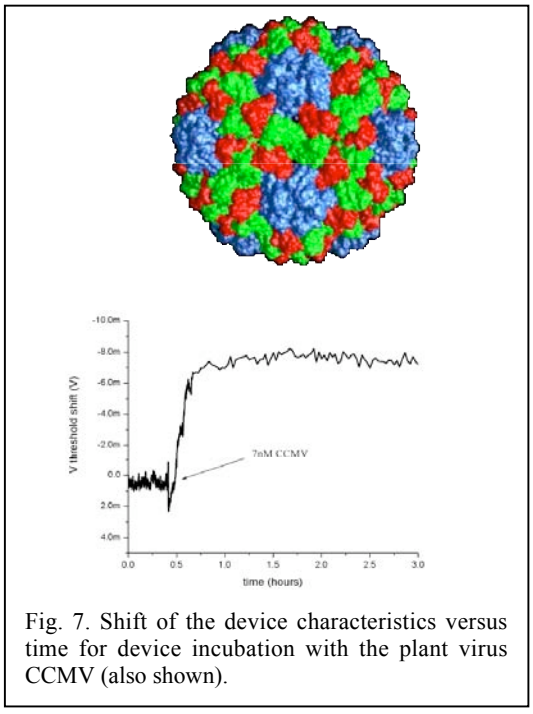

Fig. 7. Shift of the device characteristics versus time for device incubation with the plant virus CCMV (also shown).

5.2. Detection of viruses

One expects that, because of their surface proteins, viruses also readily interact with the devices and are immobilized. This has been partially confirmed by experiments using the plant virus CCMV. Just like in case of proteins one observes a shift **(Figure 7)** of the DC indicating charge transfer from the surface proteins to the device. The effect, however is surprisingly small, about an order of magnitude smaller than in case of streptavidin. It appears that binding of the surface proteins to the device is weak, and binding is also hampered by the geometric arrangement of the surface proteins due to their position within the virus structure. Moreover, it is highly virus specific, binding of the virusT4 leads to significantly smaller effect that CCMV. This, by itself is not surprising due to the significant structural and also chemical difference between the two viruses.

6. SENSING BIOLOGICAL PROCESSES USING NANOTUBE FET DEVICES.

The examples given in before illustrate the interaction between the bio-molecules and the electronic devices. The experiments summarized there give important insight into biomolecule immobilization issues, but also lay the ground work for electronic detection of biological processes. Two examples, that take the electronic detection of biological reaction concept one step further are given here: the detection of ligand-receptor binding and the detection of an enzymatic reaction.

6.1.Ligand-receptor interactions

Monitoring specific interactions between biomolecules remains one of he most important objectives of biosensing[47-49]. The detection scheme that involves electronic detection is shown in **Figure 8a**. First a polymer layer is applied to the device in order to avoid nonspecific biomolecule binding. Subsequently a ligand is attached to the layer, such ligand serves as the recognition site through ligand-receptor binding. Finally, the resulting structure is incubated with the receptor in order to explore the binding

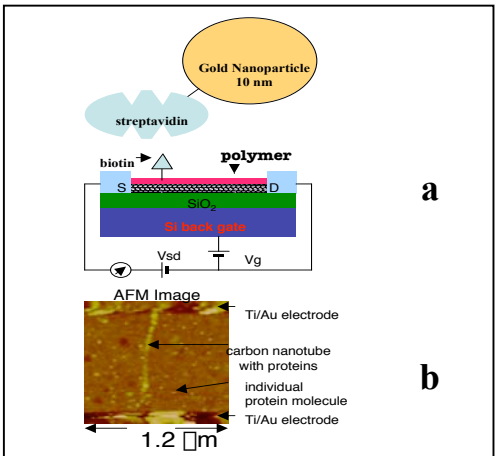

Fig.8. a) Detection scheme for biotin-streptavidin ligand receptor binding. b) AFM image of the device after incubation with gold labeled streptavidin. The vertical line with bright dots is the nanotube channel indicating streptavidin attachment, mainly to the nanotube.

process. All these steps can readily be followed by examining the device characteristics after each step. The scheme is expected to work for a broad variety of interactions, and may be appropriate even for detecting DNA duplex formation. In Ref. 14, PEI/PEG layer, biotin as the ligand and gold labeled streptavidin as the receptor was used. We have found that the PEI/PEI layer effectively prevents (in contrast to what we have found in non-functionalized nanotubes) the binding of streptavidin to the device. After polymer coating, biotin was covalently attached to the polymer and the device was subsequently incubated with gold nanoparticle-labeled streptavidin. The SEM image, shown in **Figure 8b** is the realization of the architecture, and of the end-result of the incubation process. The image clearly identifies the gold particles along the nanotube, giving evidence of streptavidin binding onto the nanotube in question. With a length of 800nm of the nanotube, and a gold sphere diameter of 10nm, it is expected that, upon full coating there are approximately 80 streptavidin molecules in direct interaction with the nanotube conducting channel, in good agreement with what one concludes through direct examination of the image. Biotin-streptavidin binding has been detected by changes in the device characteristic. The resulting change of the DC is displayed in **Fig.9a**. Instead of the shift of the DC one observes a suppression of the conduction, most likely due to some distortion of the nanotube, caused by the presence of streptavidin, such distortion leading to a carrier scattering, and thus reducing the mobility of the channel. The change exceeds the noise limit by a factor of approximately 10, leading to the conclusion that the current detection limit is about 10 proteins. Various control experiments have also been conducted. Non-specific binding was electronically detected in case of streptavidin (**Figure 6**) before, but - as discussed above - a PEI/PEG layer was found to prevent nonspecific binding, and indeed no change of the device characteristic was found when polymer-coated devices were incubated with streptavidin and other proteins (**Figure 9c**). Control experiments involving biotinilated streptavidin with the binding sites already occupied by biotin did not, as expected, result in binding. This is indicated by the fact that the device characteristics did not change upon incubation (**Figure 9b**).

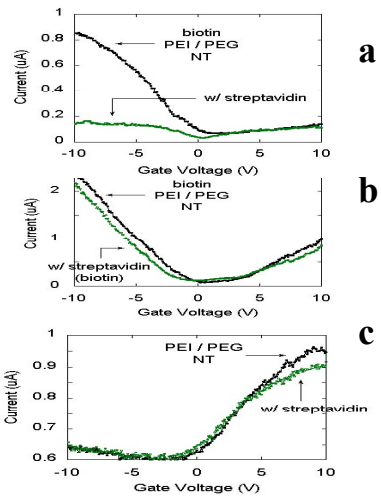

Fig 9. Ligand receptor binding between biotin and streptavidin. a) response of device illustrated on fig 1a. b) control experiment involving biotinilated streptavidin. c) control experiment using the device illustrated in Fig 1a, but without biotin attachment.

6.2. Enzymatic reactions

As an example of the application of devices for the electronic monitoring of an enzymatic reaction[50-52], the enzymatic hydrolysis of starch has been performed[53]. Starch consists of linear component, amylose which is composed of linkages between D-glucopyranose residues, and amylopectin, the branched one, which in addition to a-1,4 linked D-glucopyranose chains carry branches at C-6 on every 25 or so D-glucopyranose residues which also have the a-configuration[54]. We have characterized starch enzymatic hydrolysis with amyloglucosidase[55] in acidic buffer, resulting in complete cleavage of the polymer to water soluble glucose. Enzymatic hydrolysis of starch using amyloglucosidase in solution has been shown to be efficient in precipitating carbon nanotubes from their solution.

The starch covered single wall nanotubes (SWNT) were studied by transmission electron microscopies. **Figure 10a** shows high-resolution electron transmission (HRTEM) image of SWNT covered with starch. For imaging purposes, the starch was contrasted by using RuO_4 staining procedure. After starch deposition, the DC shifts by approximately ~ 2 volts toward negative gate voltages (**Figure 10b**) corresponding to electron doping of the nanotube channel by polymer. Compared to other polymers, such as

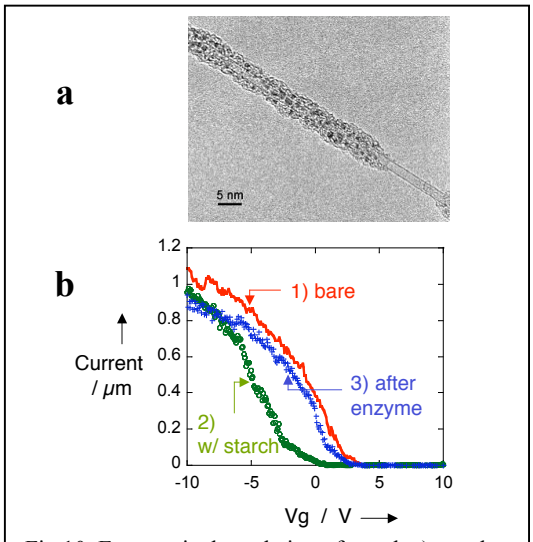

Fig.10. Enzymatic degradation of starch a) starch coated nanotube, b) device characteristics before, and after starch deposition and after the enzymatic degradation of starch.

poly(ethylene imine) (PEI), the magnitude of the shift is small. This fact, most likely, relates to difference between electron donating ability of alcohol and ether groups in starch as compare to amines in PEI. After the enzymatic reaction was completed on the starch functionalized device, the device response observed before starch deposition (**Figure 3b**) is recovered, indicating that during enzymatic reaction all the starch is hydrolized to glucose, with the hydrolization product washed off prior to the electronic measurements. Two control experiments were performed to confirm these results. First, the starch functionalized chip was rinsed with buffer to see if the buffer alone can wash away the starch deposited on the device. The DC after rinsing with buffer solution is similar to that obtained before rinsing, leading to the conclusion that starch removal by buffer alone does not occur. Another control experiment involved the deposition of enzyme solution on bare devices. The DC shows increased hysteresis but no significant shifting has been observed – giving evidence that enzyme alone does not lead to charge transfer.

7. BIO-ELECTRONIC INTEGRATION: BACTERIORHODOPSIN, BR IN A PURPLE LAYER

The next example involves a bio-entity with well defined biological function – a protein-membrane compex[56]. As the cell membrane, we have chosen the purple membrane (PM) from *Halobacterium salinarum*[57], which has been widely studied. PM contains the light-sensitive membrane protein bacteriorhodopsin, which serves as a photochemical proton pump and has been used to fabricate phototransistors. The structure is depicted in **Figure 11a**. In addition, rhodopsin has a permanent electric dipole moment, a charge distribution which produces an electric field pointing from the extracellular side of the membrane towards the cytoplasmic side[56]. These properties make PM an ideal prototype membrane for nanobioelectronic integration. In particular, we use the dipole as an indicator that the integration preserves the biomaterial while bringing it into contact with the nanoelectronic devices.

PM isolated from *Halobacterium salinarum*[57] was deposited on devices. To observe the effect of the electric dipoles fixed in the PM, devices were prepared in three conditions, as shown in **Fig. 11b**: with the cytoplasmic side of the PM facing the nanotubes[58], with the extracellular side facing the nanotubes, and with a mixture of both orientations[59]. The particular orientation was achieved by applying a gate voltage as described in **Fig 11** of +3V or –3V. Such voltage leads to electric field oriented according to the voltage polarity at the nanotube network surface. Such changes by interacting with the electric dipoles of the bR in the purple membrane are most likely responsible for the gate voltage influenced deposition.

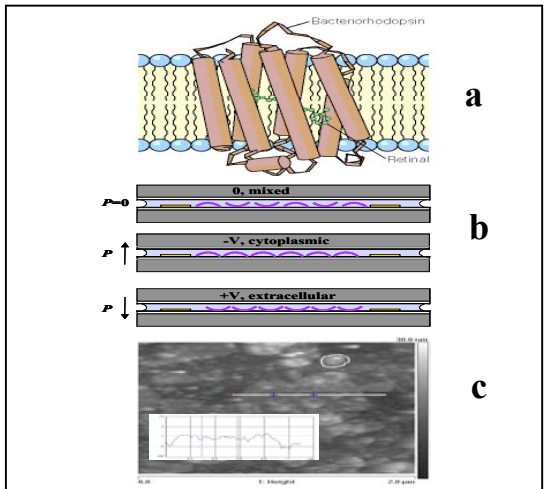

Fig 11. a). Illustration of bacteriorhodopsin in a purple membrane. b). Three purple membrane, PM arrangements, random, cytoplasmic and extracellular, deposited by employing 0, -3V and +3V voltages. The grey areas correspond to two Si chips, and the voltages were applied between the two chips. The voltages listed correspond to the potential on the top chip. c). AFM image of deposited PM, the scan indicates the height of the membrane, approximately 5nm.

The structure we have examined is a dense network of individual carbon nanotubes (**Fig. 2**) covered by the membrane, referred to as a nanotube network field-effect transistor (NTN-FET). The deposition of purple membrane has been examined by AFM imaging, such image is shown in **Fig. 11c**. One observes layers of 5nm height, corresponding to a single layer of the membrane. This configuration has several significant features. First, the cell membrane is in direct contact with the semiconducting channel of the transistor. This is distinct from previous work, in which cell membranes have contacted the gate electrodes of transistors[23]. In this configuration, transistors detect the electrical potential across membranes; in contrast, our devices detect local electrostatic charges on the biomolecules. Second, the use of a large number of nanotubes ensures that entire patches of membrane are in contact with nanotubes.

Figure 12a highlights three main device parameters before and after deposition for a typical device without the application of a voltage (resulting in a randomly oriented membrane). The changes were observed repeatedly in several devices prepared in the same way. First, the hysteresis loops narrowed significantly, as indicated by the arrows. Second, the threshold voltage changed by +1.0 ± 0.2 V, as indicated by the arrows on the x-axis. Finally, the device characteristics decreased by about 20% for negative gate voltages. These changes show that the PM has been successfully integrated with the NTN-FETs.

Next, we compare the effects of oriented PM deposition. In both orientations **(Figs. 12b and 12c)** the membrane deposition caused a narrowing of the hysteresis loops similar to that caused by the mixed-orientation deposition. At the same time, the threshold voltages shifted, in opposite directions according to the orientation of the membrane. Finally, the transconductance did not change, although the maximum conductance changed in accordance with the shifts in the threshold voltage.

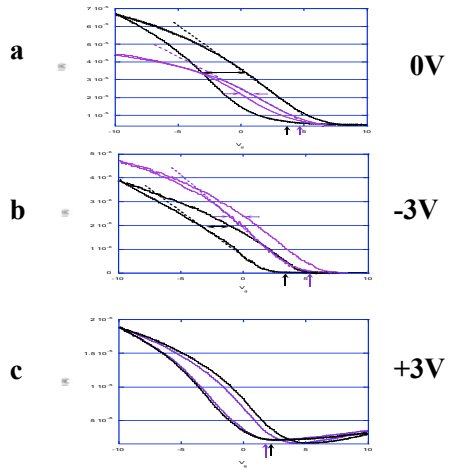

Fig. 12. a) Device characteristics for a device before (black) and after (purple) the deposition of cell membrane. Each DC has two curves, from the right-moving sweep of gate voltage and the left-moving. The intrinsic threshold voltage, indicated by black and purple arrows respectively, is the average between the two sweeps.
b) DC before (black) and after (purple) the deposition of membrane oriented with the cytoplasmic side contacting the nanotubes.
c) DC before (black) and after (purple) the deposition of membrane oriented with the extracellular side contacting the nanotubes.

First, we discuss the change of the device characteristic upon deposition of a randomly oriented membrane. This quantity is associated with the capacitance between the nanotube network, which forms the channel, and the gate; and with the mobility of carriers within the nanotube network. The capacitance is unlikely to change as a result of membrane deposition; and this is confirmed by the fact that the transconductance is not changed by oriented membrane deposition. In the case of mixed-oriented membrane deposition, the alternation of positive and negative electric dipoles on a length scale of about 500 nm (the diameter of a typical patch of PM) should act as a significant random scattering potential, which decreases the carrier mobility in the network[60]. Thus, the decrease in DC in **Fig. 12a** is a direct result of the mixture of orientations. Second, the hysteresis decreased dramatically in all cases as a result of the biological coating. The hysteresis is known to result from adsorbed water on the substrate[61]; in addition, coatings which displace water from the nanotubes reduce the hysteresis. Consequently, we expect a decrease in hysteresis here as well, presuming that the PM remains intact as a layer contacting the nanotubes. Moreover, the width of the remaining hysteresis is similar for all three conditions, which suggests that the amount of PM coverage is similar. This conclusion was confirmed in randomly selected spots that were imaged by AFM. Third, the shift of the threshold voltage in the devices results from the electrostatic field associated with the bacteriorhodopsin electric dipole. This field induces charge in the nanotubes, thus shifting the Fermi level[62]. The position of the Fermi level is measured by the threshold voltage, and prior work has established the relationship between the threshold voltage in various device configurations and the quantity of charge induced in the nanotubes[63-65]. Using these works, we have evaluated the shift caused by mixed-orientation PM deposition and find an induced charge of 16 aC/mm of nanotube length.

Several important conclusions can be reached. First, the electronic device functionality is preserved. Second, the PM remains intact as a layer, and the bacteriorhodopsin membrane proteins retain their electric dipoles. Third, the deposited PM has been demonstrated to contact the device directly and to interact with it's electrical properties.

One can also examine the significant asymmetry between cytoplasmic and extracellular orientations. This asymmetry is reflected in the large amount of charge induced in mixed-orientation devices, since without an asymmetry, the charge induced by equal amounts of cytoplasmic- and extracellular-oriented PM should cancel[66]. Such an asymmetry is known to exist, in that the dipole is closer to one side of the PM than the other[67]. Here we are able to observe this asymmetry directly because of the device configuration in which the PM contacts the nanotubes directly. One can quantify the asymmetry, by modeling the electrostatic effect of the bacteriorhodopsin dipole on the nanotubes[64] and the model is depicted in **Fig.13** Furthermore, we can quantify the asymmetry, by modeling the electrostatic effect of the bacteriorhodopsin dipole on the nanotubes[68]. The dipole is still not well understood, but it is known to result from the competition between several charge distributions that result in a net dipole moment of 3.3×10^{-28} C·m per rhodopsin monomer. To calculate the effect of this dipole on the nanotubes, we use a simple electrostatic model in which the rhodopsin molecules above a nanotube (**Fig. 13**) form a line of constant dipole density. In this model, the line of dipoles

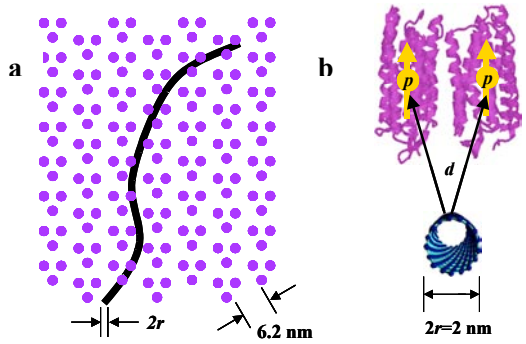

Fig 13. a. Model illustrating the geometry of PM with respect to the nanotubes. Rhodopsin (purple dots) assembles into trimers, which are arranged on a hexagonal lattice. The nanotube is a curved line. b. Model illustrating the dimensions used in the calculations. A rhodopsin monomer situated near a nanotube has a dipole moment p. This point dipole is situated within the rhodopsin at a distance d from the nanotube surface.

with a density σ induces a charge density, σ, given by $\sigma = \sigma r \sigma / d^2$. Thus, by combining the known dipole moment of bacteriorhodopsin with the induced charge (measured from the threshold voltage shift and the known capacitance), we calculate how far the dipoles lie from the nanotubes. The answer will be different for the two different orientations, reflecting the position of the dipoles closer to one side of the PM. For the cytoplasmic orientation, with $\Delta V_{cp} = +2.2$ V, $d_{cp} = 1.9$ nm. For the extracellular orientation, with $\Delta V_{ec} = -0.4$ V, $d_{ec} = 4.4$ nm. Since the sum of these distances, 6.3 nm, is comparable to the membrane bilayer thickness of 5 nm[34], we conclude that this simple model is reasonable. Note, in particular, that since the ratio between ΔV_{cp} and ΔV_{ec} is 5.5, the electrostatic model indicates that d_{cp} is 2.3 times smaller than d_{ec}. Thus, our data contribute additional details about the asymmetry of the bacteriorhodopsin charge distribution.

8. CONCLUSIONS

The nanoscale electronic devices – field effect transistors with carbon nanotube conducting channels– we have fabricated interact readily with the environment. For a variety of species, such as reactive gases, polymers with reactive chemical groups and also for proteins and viruses that have been studied our experiments demonstrate that charge transfer occurs between the species and the devices. The change of the device characteristics, DC allows the estimation of the transferred charge for each species. Our observations in case of proteins also suggest strong charge transfer from the protein to the nanotube channel. The charge transfer interaction mechanism we have identified for proteins may have implications on a broad range of areas where immobilization is attempted and used for fundamental studies and also for applications. Such interactions also involve functional groups different from those involved in hydrophobic interactions, and thus may lead to different attachment geometries in the two cases. Experiments involving a variety of proteins may shed light on some of the issues raised in here.

In conclusion, enough is now known about nanoelectronics that we are able to use a nanodevice as an investigative tool. One can use these devices for monitoring a variety of biologically significant reactions. This is possible because most of such reactions involve local electric fields and also charge rearrangement. We have also used the interaction between a biological system and a nanodevice not to learn about the electronic component, but to learn about the biological component. As a result, it should be possible to connect living cells directly to these nanoelectronic devices. The stage is set for the next phase of nanotechnology research.

The above concepts could conceivably be extended at a later stage to include of what one could call “cellectronics”, cell-based electronic sensing: measuring the electronic response of living systems, and to using nanoscale devices for in-vivo applications: studying cell physiology, medical screening and diagnosis. The sensor architectures can be turned into devices where – by applying a voltage between elements of the sensor – surface charges can be created on the sensing element where the bio-molecules are immobilized. Such surface charges will interact with the charged bio-molecules, but such, potentially important effects have not been explored to date. The small size of the nanotube devices also allows the integration of the devices into living organisms. This will allow in-vivo electronic detection of biological processes.

ACKNOWLEDGEMENTS

The experiments reported here were performed by K. Bradley, A. Star, J.C. Gabriel and A. Davis. They also contributed to the development of concepts in the area of nano-bioelectronic interface. This work was also supported by the NSF grant, 0415130.

REFERENCES

1. M. Robers. I.J.A.M. Rensink, C.E. Hack, L.A. Aarden, C.P.M. Reutelingsperger, J.F.C. Glatz and W.T. Hermens , "A new principle for rapid immunoassay of proteins based on in situ precipitate-enhanced ellipsometry". Biophysical Journal. **76**, pp 2769-2776 (1999)
2. C.J, McNeil, D. Athey, On Ho Wah, "Direct electron transfer bioelectronic interfaces: application to clinical analysis", Biosensors & Bioelectronics **10**, pp.75-83 (1995)
3. I. Willner, "BIOELECTRONICS: Biomaterials for Sensors, Fuel Cells, and Circuitry", Science **298**, 2407 (2002).
4. H. Hu, Y. Ni, V. Montana, R. C. Haddon, V. Parpura, "Chemically Functionalized Carbon Nanotubes as Substrates for Neuronal Growth", Nano Letters **4**, 507 (2004).
5. D. Pantarotto, C. D. Partidos, R. Graff, J. Hoebeke, J.-P. Briand, M. Prato, A. Bianco, "Synthesis, Structural Characterization, and Immunological Properties of Carbon Nanotubes Functionalized with Peptides", J. Am. Chem. Soc. **125**, 6160 (2003).
6. Ming Zheng, Anand Jagota, Michael S. Strano, Adelina P. Santos, Paul Barone, S. Grace Chou, Bruce A. Diner, Mildred S. Dresselhaus, Robert S. Mclean, G. Bibiana Onoa, Georgii G. Samsonidze, Ellen D. Semke, Monica Usrey, and Dennis J. Walls, "Structure-Based Carbon Nanotube Sorting by Sequence-Dependent DNA Assembly", Science **302**, 1545 (2003).
7. Cyrille Richard, Fabrice Balavoine, Patrick Schultz, Thomas W. Ebbesen, and Charles Mioskowski, "Supramolecular Self-Assembly of Lipid Derivatives on Carbon Nanotubes", Science **300**, pp 775-778 (2003).
8. M. Shim, N. W. Shi Kam, R. J. Chen, Y. Li, H. Dai, "Functionalization of Carbon Nanotubes for Biocompatibility and Biomolecular Recognition", Nano Lett. **2**, pp 285-288 (2002)
9. W. Huang, S. Taylor, K. Fu, Y. Lin, D. Zhang, T. W. Hanks, A. M. Rao, Y.-P. Sun, "Attaching Proteins to Carbon Nanotubes via Diimide-Activated Amidation", Nano Lett. **2**, pp 311-314 (2002)
10. R. J. Chen, Y. Zhang, D. Wang, H. Dai, "Noncovalent Sidewall Functionalization of Single-Walled Carbon Nanotubes for Protein Immobilization", J. Am. Chem. Soc. **123**, pp 3838-3839 (2001)
11. Jason J. Davis, Malcolm L. H. Green, H. Allen O. Hill, Yun C. Leung, Peter J. Sadler, Jeremy Sloan, Antonio V. Xavier and Shik Chi Tsang, "The immobilisation of proteins in carbon nanotubes", Inorganica Chimica Acta **272**, pp 261-266 (1998)
12. F. Balavoine, P. Schultz, C. Richard, V. Mallouh, T.W. Ebbesen, C. Mioskowski, "Helical crystallization of proteins on carbon nanotubes: A first step towards the development of new biosensors", Angew. Chem. Int. Ed. **38**, pp 1912-1915. (1999)
13. G. R. Dieckmann, A. B. Dalton, P. A. Johnson, J. Razal, J. Chen, G. M. Giordano, E. Munoz, I. H. Musselman, R. H. Baughman, R. K. Draper, "Controlled Assembly of Carbon Nanotubes by Designed Amphiphilic Peptide Helices", J. Am. Chem. Soc. **125**, pp 1770-1777 (2003)
14. R. Martel, T. Schmidt, H. R. Shea, T. Hertel, and Ph. Avouris, "Single- and multi-wall carbon nanotube field-effect transistors", Appl. Phys. Lett. Vol. 73, pp2447-2449, (1998)
15. Adrian Bachtold, Peter Hadley, Takeshi Nakanishi, and Cees Dekker, "Logic Circuits with Carbon Nanotube Transistors", Science 294, pp1317-1320 (2001)
16. Philip G. Collins, Keith Bradley, Masa Ishigami, A. Zettl, "Extreme Oxygen Sensitivity of Electronic Properties of Carbon Nanotubes", Science 287, pp1801-1804 (2000)
17. Jing Kong, Nathan R. Franklin, Chongwu Zhou, Michael G. Chapline, Shu Peng, Kyeongjae Cho, and Hongjie Dai, "Nanotube Molecular Wires as Chemical Sensors", Science 287, pp 622-625 (2000)
18. Alexander Star, Tzong-Ruhan, Jean-Christophe P. Gabriel, Keith Bradley, and George Grüner, "Interaction of Aromatic compounds with Carbon nanotubes", Nano Lett. 3, pp 1421-23 (2003)
19. Keith Bradley, Jean-Christophe P. Gabriel, Mikhail Briman, Alexander Star, George Grüner, "Charge transfer from aqueous ammonia absorbed on nanotube transistors", Phys. Rev. Lett. 91, pp 218301-04 (2003)
20. Yi Cui, Qingqiao Wei, Hongkun Park, and Charles M. Lieber, "Nanowire Nanosensors for Highly Sensitive and Selective Detection of Biological and Chemical Species", Science 293, pp1289-1292 (2001)
21. Keith Bradley, Mikhail Briman, Alexander Star, and George Grüner, "Charge Transfer from Adsorbed Proteins", Nano Lett. 4, pp 253-256 (2004)
22. A. Star, , K. Bradley, J.-C. P. Gabriel, G. Grüner, "Nano-Electronic Sensors: Chemical Detection Using Carbon Nanotubes", Pol. Mater.: Sci. Eng. 89, pp 204 (2003)
23. K. Bradley J.-C. P. Gabriel, A. Star and G. Grüner, "Short Channel Effects in contact-passivated nanotube chemical sensors", Appl. Phys. Lett., 83, pp 3821-23 (2003)

24. Delmar S. Larsen, Kaoru Ohta, Qing-hua Xu, Michelle Cyrier, and Graham R. Fleming, "Influence of Intramolecular Vibrations in Third-Order, Time Domain Resonant Spectroscopies: 1. Experiments", Journal of Chemical Physics 114, pp 8008-8019 (2001).
25. A. Xie, A. F. G. van der Meer, R. H. Austin, "Excited-State Lifetimes of Far-Infrared Collective Modes in Proteins", Phys. Rev. Lett. 88, pp 018102 (2002)
26. Arai M, Ikura T, Semisotnov GV, Kihara H, Amemiya Y, Kuwajima K. , "Kinetic Refolding of Beta-lactoglobulin. Studies by Synchrotron X-ray Scattering, and Circular Dichroism, Absorption and Fluorescence Spectroscopy", J. Mol. Biol. 275, pp149-162. (1998)
27. L. Pollack, M. W. Tate, A. C. Finnefrock, C. Kalidas, S. Trotter, N. C. Darnton, L. Lurio, R. H. Austin, C. A. Batt, S. M. Gruner, and S. G. J. Mochrie, "Time Resolved Collapse of a Folding Protein Observed with Small Angle X-Ray Scattering," Phys Rev Lett 86, pp 4962-4965 (2001)
28. Kazuo Kuwata, Ramachandra Shastry, Hong Cheng, Masaru Hoshino, Carl A. Batt, Yuji Goto, Heinrich Roder, "Structural and kinetic characterization of early folding events in –lactoglobulin", Nature Struct Biol 8, pp.151 - 155 (2001)
29. C.M. Jones, E.R. Henry, Y. Hu, C. Chan, S.D. Luck, A. Bhuyan, H. Roder, J. Hofrichter, and W.A. Eaton, "Fast Events in Protein Folding Initiated by Nanosecond Laser Photolysis", PNAS 90, pp.11860-11864 (1993)
30. M. Lim, T. A. Jackson, P. A. Anfinrud, "Modulating carbon monoxide binding affinity and kinetics in myoglobin: the roles of the distal histidine and the heme pocket docking site", J. Biol. Inorg. Chem. 2, pp. 531 – 536 (1997)
31. E.A.Lipman, B.Schuler, O.Bakajin and W.A.Eaton, "Single molecule Measurement of Protein Folding", Kinetics 310, pp1233 (2003)
32. Rosenblatt, S.,Yaish, Y., Park, J., Gore, J., Sazonova, V., McEuen, P. L., "High Performance Electrolyte Gated Carbon Nanotube Transistors", Nano Lett., 2, pp 869-872 (2002)
M. Krüger, M. R. Buitelaar, T. Nussbaumer, C. Schönenberger and L. Forró, "Electrochemical carbon nanotube field-effect transistor", Appl. Phys. Lett., 78, pp. 1291-1293 (2001)
33. H. Chang, J. D. Lee, S. M. Lee, and Y. H. Lee, "Adsorption of NH3 and NO2 molecules on carbon nanotubes", Appl. Phys. Lett., 79, pp 3863-3865 (2001)
34. Jing Kong and Hongjie Dai, "Full and Modulated Chemical Gating of Individual Carbon Nanotubes by Organic Amine Compounds", J. Phys. Chem. B 105, pp 2890 – 2893 (2001)
35. M. Robers, I. J. A. M. Rensink, C.E. Hack, L.A. Aarden, C.P.M. Reutelingsperger, J.F.C. Glatz, and W,T. Hermens, "A new principle for rapid immunoassay of proteins based on in situ precipitate-enhanced ellipsometry",. Biophysical Journal. 76, pp 2769-2776 (1999)
36. C.J. McNeil, D. Athey and W.O. Ho, "Direct electron transfer bioelectronic interfaces: application to clinical analysis", Biosens. Bioelectron. 10, pp.75-83 (1995)
37. D.C. Turner, C.Y. Chang, K. Fang, S.L. Brandow and D.B. Murphy, "Selective adhesion of functional microtubules to patterned silane surfaces", Biophysical Journal 69, pp.2782-9 (1995)
38. K. Wadu-Mesthrige, N. A. Amro, J. C. Garno, S. Xu, and G.-Y. Liu, "Fabrication of nanometer-sized protein patterns using atomic force microscopy and selective immobilization", Biophys. J. 80, pp1891-1899 (2001)
39. D. V. Nicolau, T. Taguchi, H. Taniguchi, and S. Yoshikawa, "Micron-Sized Protein Patterning on Diazonaphthoquinone/Novolak Thin Polymeric Films", Langmuir 14, pp1927-1936 (1998)
40. P. P. Pompa, L. Blasi, L. Longo, R. Cingolani, G. Ciccarella, G. Vasapollo, R. Rinaldi, A. Rizzello, C. Storelli, and M. Maffia, Phys. Rev. E 67, pp 41902-1-8 (2003)
41. G. Sagvolden, "Protein adhesion force dynamics and single adhesion events ", Biophys. J. 77, pp 526-532 (1999)
42. P. C. Weber, J. J. Wendoloski, M. W. Pantoliano, and F. R. Salemme, "Crystallographic and thermodynamic comparison of natural and synthetic ligands bound to streptavidin ", J. Am. Chem. Soc. 114, pp 3197-3200 (1992)
43. F. K. Athappilly, W. A. Hendrickson, "Crystallographic analysis of the pH-dependent binding of iminobiotin by streptavidin ", Protein Sci. 6, pp 1338-1342 (1997)
44. M. T. Yatcilla, C. R. Robertson, A. P. Gast, "Influence of pH on Two-Dimensional Streptavidin Crystals ", Langmuir 14, pp 497-503 (1998)
45. S.-W. Wang, C. R. Robertson, A. P. Gast, "Role of N- and C-Terminal Amino Acids in Two-Dimensional Streptavidin Crystal Form", Langmuir 16, pp 5199-5204 (2000)
46. W. Frey, W. R., Schief Jr., D. W. Pack, C.-T. Chen, A. Chilkoti, P. Stayton, V. Vogel, F. A. Arnold, "Two-dimensional protein crystallization via metal-ion coordination by naturally occurring surface histidines ", Proc. Natl. Acad. Sci. U.S.A., 93, pp 4937-4941 (1996)A. Star, J.-C.P. Gabriel, K. Bradley, G. Grüner, "Electronic Detection of Specific Protein Binding Using Nanotube FET Devices ", Nano Lett. 3, pp 459-463 (2003)

47. A. Star, J.-C.P. Gabriel, K. Bradley, G. Grüner, "Electronic Detection of Specific Protein Binding Using Nanotube FET Devices ", Nano Lett. **3**, pp 459-463 (2003)
48. R.J. Chen, S. Bangsaruntip, K.A. Drouvalakis, N. Wong Shi Kam, M. Shim, Y. Li, W. Kim, P. J Utz,. H. Dai, "Noncovalent functionalization of carbon nanotubes for highly specific electronic biosensors", Proc. Natl. Acad. Sci. USA 100, pp 4984-4989 (2003)
49. K. Besteman, J.-O. Lee, F.G.M. Wiertz, H.A. Heering, C. Dekker, "Enzyme-Coated Carbon Nanotubes as Single-Molecule Biosensors", Nano Lett. 3, pp 727-730 (2003)
50. W. Schnabel, Polymer Degradation, Chapter 6, Henser International: Berlin, 1981.
51. R. P. Wool, D. Raghavan, G. C. Wagner, S. J. Billieux, "Biodegradation Dynamics of Polymer-Starch Composites", Appl. Polym. Sci. 77, pp 1643-1657 (2000)
52. M. V. Moreno-Chulim, F. Barahona-Perez, G. Canche-Escamilla, "Biodegradation of starch and acrylic-grafted starch by Aspergillus niger", Appl. Polym. Sci. 89, pp 2764-2770 (2003)
53. A. Star, V. Joshi, T.-R. Han, M. V. P. Altoe, G. Gruner, J. F.Stoddart,, "Electronic Detection of the Enzymatic Degradation of Starch ", Org. Lett. 6, pp 2089-2092 (2004)
54. P. Collins, R. Ferrier, Polysaccharides: Their Chemistry, pp. 478-523, John Wiley & Sons, Chichester, 1995 (b) J. Lehmann, Carbohydrates: Structure and Biology, pp. 98-103, Georg Thieme Verlag, Stuttgart, 1998 (c) D.B. Thompson, "On the non-random nature of amylopectin branching", Carbohydr. Polym. 43, pp 223-239 (2000)
55. T. Yamamoto, Enzyme Chemistry and Molecular Biology of Amylases and Related Enzymes, pp. 3-201, CRC press, Inc. 1995,
56. K. Bradley, A. Davis, J-C. P. Gabriel and G. Gruner, " Nanobioelectronics: integration of cell membranes and nanotube transistors (to be published)
57. D. Oesterhelt, and W., Stoeckenius, "Functions of a New Photoreceptor Membrane ", Proc. Natl. Acad. Sci. U.S.A. 70, pp 2853-2857 (1973)..
    H.J. Steinhoff, R. Mollaaghababa, C. Altenbach, K. Hideg, M. Krebs, H.G. Khorana, W.L. Hubbell, "Time-resolved detection of structural changes during the photocycle of spin-labeled bacteriorhodopsin", Science 266, pp 105-107 (1994).
58. G. Várò, Acta Biol. Acad. Sci. Hung. 32, 301 (1981)..
59. . Yi Shen, Cyrus R. Safinya, Keng S. Liang, A. F. Ruppert, Kenneth J. Rothschild, "Stabilization of the membrane protein bacteriorhodopsin to 140 °C in two-dimensional films", Nature 366, pp 48-50 (1993).
    K. Koyama, N. Yamaguchi, and T. Miyasaka, "Antibody-mediated bacteriorhodopsin orientation for molecular device architectures", Science 265, pp 762-765 (1994)
60. . Sander J. Tans, Cees Dekker, "Molecular transistors: Potential modulations along carbon nanotubes ", Nature 404, pp 834-835 (2000).
61. K. Bradley, J. Cumings, A. Star, J.-C. P. Gabriel, G. Gruner, "Influence of Mobile Ions on Nanotube Based FET Devices", Nano Lett. 3, pp 639-641 (2003)
62. M. Freitag, M. Radosavljevic, Y. Zhou, A. T. Johnson, W. F. Smith, "Controlled creation of a carbon nanotube diode by a scanned gate", App. Phys. Lett. 79, pp 3326-3328 (2001).
63. Marc Bockrath, David H. Cobden, Paul L. McEuen, Nasreen G. Chopra, A. Zettl, Andreas Thess, and R. E. Smalley, "Single-Electron Transport in Ropes of Carbon Nanotubes", Science 275, pp1922-1925 (1997).
64. Ali Javey, Hyoungsub Kim, Markus Brink, Qian Wang, Ant Ural, Jing Guo, Paul McIntyre, Paul McEuen, Mark Lundstrom, Hongjie Dai, "High- dielectrics for advanced carbon-nanotube transistors and logic gates", Nature Mat. 1, pp 241-246 (2002).
65. K. Bradley, J-C P. Gabriel, M. Briman, A. Star, and G. Grüner, "Charge Transfer from Ammonia Physisorbed on Nanotubes ", Phys. Rev. Lett. 91, pp 218301 (2003).
66. This assumption, that the mixed-orientation film contains equal amounts of cytoplasmic and extracellular orientations, is justified by our AFM images.
67. B. Ehrenberg, and Y. Berezin, "Surface potential on purple membranes and its sidedness studied by a resonance Raman dye probe, Biophys. J., 45, pp 663-670 (1984)
68. The background charge due to the phosphate heads of the lipids is 0.2 electrons per square nanometer (24), which is too weak to explain the charge induced in our devices.